Ionization Dynamics for Atomic and Molecular Ions in Relativistic, Ultrastrong Laser Fields

Journal of Physics: Conference Series **2494** (2023) 012018 doi:10.1088/1742-6596/2494/1/012018

Ionization Dynamics for Atomic and Molecular Ions in Relativistic, Ultrastrong Laser Fields

B C Walker, E C Jones, Z Andreula, M Pham, M Gale, E Pedlow, A Stein

Physics and Astronomy, University of Delaware, 104 The Green, Newark, DE, USA

E-mail: bcwalker@udel.edu

Abstract. The discovery of laser-driven rescattering and high harmonic radiation out to a maximum photon energy of 3.17 times the ponderomotive energy (U_p) laid the groundwork for attosecond pulse generation and coherent X-rays. As the laser field drives the interaction to higher energies, relativity and the Lorentz force from the laser magnetic field enter into the dynamics. We present the results of recent studies of laser rescattering, including these effects, to give a quantitative description of rescattering dynamics in the high-energy limit, ie, recollision energies of order 1,000 hartree (27 keV). The processes investigated include inner K- and L-shell excitation and the ultimate limit of high harmonic generation via rescattering bremsstrahlung. The results indicate the path to the frontier area of x-ray strong field processes.

1. Introduction

Strong field rescattering interactions historically were treated in the dipole approximation, neglecting the laser magnetic field [1]. As laser technology [2] continued to advance, the force from the laser magnetic field affected the dynamics [3]. A Lorentz rescattering parameter [4] was able to differentiate traditional dipole strong-field atomic and molecular interactions and the ultrastrong field regime, where the full laser electric and magnetic field is required to describe the rescattering physics. Recently, an ultimate energy limit of rescattering [5] was discovered. This energy maximum for laser-driven rescattering is approximately one-thousand Hartree (27 keV), which means laser-driven rescattering can excite atomic systems across the periodic table from hydrogen to uranium [6, 7].

We describe here laser-driven rescattering processes at the strong field and ultrastrong field ultimate energy limit boundary [4]. Specifically, we address the ability of laser-driven rescattering to excite all the bound states in naturally occurring atomic species. In addition, we show rescattering using relativistic dynamics can give laser-driven high harmonic generation with yields out to one-thousand Hartree that are higher than the traditional, strong field high harmonic generation (HHG) in neon. These two processes are described in Fig. 1 for the rescattering inner shell excitation with the L- and K-shells for atoms and in Fig. 2 for rescattering driven high harmonic radiation in the high energy, bremsstrahlung limit. In these two figures, the common foundation is clear. Tunneling field ionization of a state with an ionization energy of E_{IP} (step '1' in the figures) by a strong laser field (electric field magnitude E_0, wavelength λ, and frequency ω) creates electron density in the continuum. These electrons are then accelerated by the laser field (step '2') and can re-interact with the parent ion (step '3' in the figures) by

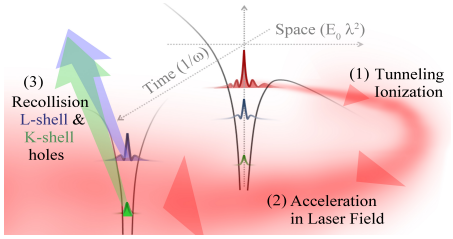

Figure 1. Sequence of (1) tunneling ionization (red) of the outermost electron, (2) laser acceleration of the photoelectron over length scale of E_0 λ^2, (3) electron return on a time scale of $1/\omega$ to the parent ion where recollision creates K- (green) and L-shell RSI (blue).

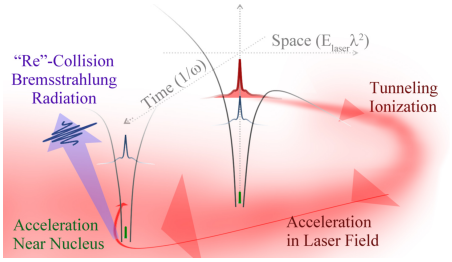

Figure 2. Visual representation of sequence from tunneling ionization (red) for the outermost electron, acceleration in the external laser field, and rescattering with the parent ion potential by the bremsstrahlung process with deflection of the rescattering.

either collisionally exciting the inner-most electrons in atoms (Fig. 1) or inelastically scatter off the nucleus with an atomic number Z (Fig. 2) to give laser-driven bremsstrahlung. Though the initial laser-driven rescattering steps in Fig. 1 and Fig. 2 are mechanistically the same, the optimum laser parameters differ. We present here the optimum laser conditions to achieve laser-driven rescattering inner shell excitation and rescattering high harmonic generation. The comparison by looking at these together shows that rescattering physics is generally possible for all atoms and ions across the periodic table. Furthermore, we show strong field x-ray interactions are key to realizing these new high-energy rescattering processes.

2. Rescattering Inner Shell Excitation

In this work, we use the semiclassical trajectory ensemble method [8, 9]. Briefly, bound state ionization is calculated by tunneling [10] and the space-time relativistic photoelectron is modeled semiclassically with a 10^4 trajectory Monte-Carlo ensemble having a position and momentum spread matched to the tunneling wave function probability as it appears in the continuum. Trajectories that return to the parent ion are counted as the rescattering fluence, F (dimension of charge/area) with the tunneling rate and the energy-resolved probability of return calculated from the trajectories [4] comprising the energy-resolved rescattering electron fluence, dF/dE, (charge/(area energy)). Connecting back to Fig. 1 and Fig. 2, the rescattering fluence dF/dE is indicated in red as the electron probability after ionization. For the recollision interaction with the parent ion (step 3) to create inner shell holes or bremsstrahlung, dF/dE is evaluated when it returns, i.e. at the spatial coordinate of the parent ion.

The energy resolved rescattering electron fluence, dF/dE, and field free K- and L_I-shell cross sections [11] are used to calculate rescattering shell ionization. Figure 3 displays an example of the energy-resolved rescattering fluence dF/dE and K-shell cross section σ. The overlap (i.e. the σ dF/dE product) gives the yield for the ejected inner shell electron as well as the excess energy shared between the outgoing electrons. The figure typifies results at the edge of the non-relativistic strong field ($\Gamma_R = 1$) with a 3.17 U_p cutoff of 110 hartree (3 keV). This energy is sufficient to ionize the carbon K-shell with a cross section threshold at $\sim$ 10 hartree (284 eV). The created photoelectron yield $\sigma(dF/dE)$ ranges from 10^{-12} electrons/hartree near threshold ($\sim$ 0 eV) to 10^{-9} electrons/hartree for photoemission with kinetic energies near 100 hartree.

Rescattering shell ionization (RSI) across the periodic table is a complex process. For this reason, we calculated K- and L_I-shell excitation for different ion species interacting with many

laser conditions. Using this exhaustive approach we were able to find maximum yields for atoms at different intensities, wavelengths, and ionization state. To maintain the integrity of the inner shell state and cross sections, we impose a limit on the ionization progression. Generally, the species chosen for this analysis favor final ion states with configurations in the upper p sub-shell of the next full shell, e.g. a principle quantum number n=3 for the L-shell.

RSI is limited from a low energy side whenever the energy is insufficient to reach the minimum required by the cross-section threshold, e.g. 284 eV (10 hartree) in Fig. 3 to remove the 1s electron for the carbon K-shell. On the high energy side, production is limited by the relativistic rescattering deflection ($\Gamma_R > 1$). The K-shell for xenon ($k_{\alpha 2} = 29,458eV$) is at the approximately one-thousand hartree limit beyond which rescattering yields drop when $\Gamma_R > 1$. For heavier nuclei ($54 < Z < 92$) it is still possible to extend the rescattering energy by a factor of a few (e.g. from 1,000 hartree to 3,500 hartree) to reach uranium ($k_{\alpha 2} = 94,665eV$) by a careful choice of the laser wavelength and intensity.

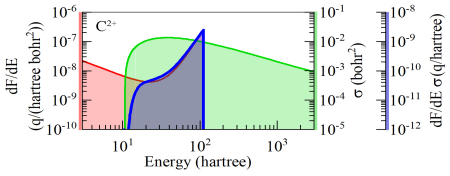

Figure 3. Energy resolved recollision flux, dF/dE (red), for C^{2+} at 4.9 μm and a peak intensity of 4×10^{14} W/cm^2. Also plotted are the inelastic cross sections σ (green) [11]. The dF/dE σ product, which contributes K-shell RSI (blue), is shown tied to the rightmost y-axis.

From our analysis of atoms and ions across the periodic table we have determined the laser fields that give a maximum in the K- and L_I-shell yields, shown for specific K-shell examples in Table I. As the atomic species studied cross the $\Gamma_R > 1$ boundary, the RSI yields continue to trend similar to the nonrelativistic interaction. This results from the optimal field solutions emphasizing the yield and trading off other physical options (such as ω, Q, E_{IP}) to limit high Γ_R solutions. At these ideal laser conditions for RSI, one can observe the yields equal the peak inner shell cross section times a fluence that is independent of Z. The yield for the K- and L_I-shell is 10^{-4} σ and 10^{-3} σ, respectively.

Table 1. Optimal laser parameters for rescattering driven K-shell ionization

Parent	I (W/cm^2)	λ(nm)	$\frac{K-Holes}{Ions}$	Γ_R	Γ_K
${}_3Li^{+}$	7×10^{14}	10,400	8.1×10^{-5}	0.01	0.21
${}_6C^{3+}$	2×10^{15}	1,200	5.4×10^{-6}	0.04	0.29
${}_{10}Ne^{4+}$	2×10^{16}	640	3.3×10^{-7}	0.18	0.24
${}_{14}Si^{5+}$	1.3×10^{17}	390	4.6×10^{-8}	0.22	0.42
${}_{18}Ar^{9+}$	1.9×10^{18}	133	2.8×10^{-8}	0.55	0.26
${}_{29}Cu^{20+}$	1.4×10^{20}	25.3	7.0×10^{-9}	0.88	0.32
${}_{36}Kr^{27+}$	7×10^{20}	13.8	3.4×10^{-9}	1.1	0.35
${}_{54}Xe^{45+}$	1.3×10^{22}	4.69	4.9×10^{-10}	2.1	0.37
${}_{74}W^{69+}$	1.5×10^{23}	1.83	1.3×10^{-10}	2.9	0.43
${}_{92}U^{83+}$	4.6×10^{23}	1.33	1.9×10^{-11}	4.9	0.41

A simple physical picture emerges in the high energy, strong field rescattering optimization. First, are the ionization energy and charge for a parent ion (with an overall ion charge $Q-1$ and ion core Q binding the ionizing electron charge). Together these largely determine the peak laser field interacting with the atom or ion. For the sake of simplicity, the peak interacting laser field can be estimated using classical barrier suppression ionization, $E_{bsi} = \frac{E_{IP}^2}{4Q}$. A second insight is a matching of the rescattering energy to the maximum in the atomic cross-section. The rescattering fluence peaks at the maximum return energy (see Fig. 3), which for $\Gamma_R \leq 1$ is ~3.2 times the quiver, or ponderomotive, energy, $U_p = E_{bsi}^2/(4\omega^2)$. Coincidentally, the characteristic inner shell cross-section peaks at ~3 times the cross-section threshold for energies below the pair creation energy. The maximum yield occurs when the fluence and cross-section peaks overlap; the greatest rescattering inner-shell ionization occurs when U_p is approximately equal to the threshold for the inner shell predicted by Moseley's law as $1/2(Z-1)^2$. Therefore, the ideal laser frequency is $\omega = E_{IP}/(\sqrt{32}\ Q\ (Z-1))$. Finally, optimal RSI occurs for $\Gamma_R \leq 1$. The criteria described above combine to give a way to determine the ideal laser conditions for high-energy rescattering. With an adjustment in the second step, the analysis can be extended to any physical process to find the optimized conditions for laser rescattering. The scaling of RSI with Z and the laser wavelength λ can also be explained [6] by analyzing the atomic inner shell cross-section Z dependence [11] and rescattering laser physics.

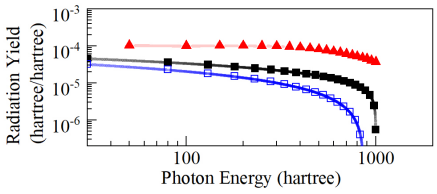

Figure 4. Bremsstrahlung yields between classical non-relativistic (blue, empty square), relativistic-numerical (red, triangle), and Bethe-Heitler (black, square) formulations for a 1000 hartree electron flux incident on uranium.

3. Ultimate Limit of Rescattering Bremsstrahlung, High Harmonic Generation

Recollision as a process extends up to an ultimate limit for the acceleration and rescattering energy [4, 5] of order one-thousand hartree. Electrons at one-thousand hartree have a DeBroglie wavelength ($\lambda_{deBroglie} = h/p$) of 0.14 bohr, where a classical approach [12] can be considered valid for many atomic and molecular interactions. Viewing recollision in the classical regime is also consistent with the large $\sim e|E_0|/(m_0\omega^2)$ excursion distance for the photoelectron (charge e, mass m_0) as it is driven by the laser field. Inelastic rescattering with the parent ion can create (e,ne) [13, 14, 15] secondary electrons, or HHG radiation.

We model the HHG radiation process as a bremsstrahlung mechanism with the recollision occurring as the returning electron is accelerated by the parent ion potential. All presented results are in the single atom response limit and use plane wave radiation for the laser field. We consider both the bare nucleus, where the interaction is between the incoming electron and the full nuclear charge, and scattering from the ion core shielded nucleus in the approximation of a center-symmetric representation for the bound electrons [16]. The scattering process is calculated using classical, numerical-relativistic, and relativistic quantum [17] treatments for bremsstrahlung.

Calculations of rescattering bremsstrahlung yields as a function of the bremsstrahlung photon energy (hartree/hartree dimension for a single atom or ion) use a general formulation given by,

$$E_{brem}(E_\gamma) = \int \tilde{F_R}(E_r)\frac{d^2\chi(E_r, E_\gamma)}{dE_\gamma}dE_r \quad (1)$$

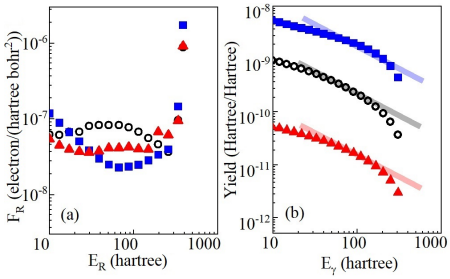

Figure 5. Numerical rescattering flux (a) and bremsstrahlung yields (b) given by Eq. 1 with $\Gamma_R = 1$ for U^{14+} (square, blue) at 304nm and 3.9×10^{17} W/cm^2, Kr^{8+} (open circle, black) at 409nm and 2.2×10^{17} W/cm^2, and Ne^{5+} (triangle, red) at 409nm and 2.2×10^{17} W/cm^2. Reference lines are projected onto (b) to indicate Z^2 scaled yields for U and Kr based on the relative yield from Ne.

where $\tilde{F_R}(E_r)$ is a generalized rescattering flux (electron/(energy-area) dimension) as a function of the rescattering energy E_r. This is the same energy-resolved rescattering fluence indicated in Fig. 1, Fig. 2, shown by way of example in Fig. 3, and used in the calculations of rescattering inner shell ionization of the previous section. The bremsstrahlung generation is sourced in $\chi(E_r, E_\gamma)$, which represents the generalized energy cross-section ((energy-area)/electron dimension) as a function of E_r (again, the energy of the rescattering electron) and photon energy E_γ. Integrating Eq. 1 over E_γ gives the radiated energy per photon interval. The functions for $\chi(E_r, E_\gamma)$ are well known for each of the approximations used in the calculations, i.e. classical, numerical relativistic classical scattering, and relativistic quantum. For brevity, we will refer the reader to [7] for the full derivations and focus here on two essential findings.

First is addressing the ability of classical, non-relativistic calculations to model the rescattering bremsstrahlung process near the ultimate energy limit. The accuracy of the classical, non-relativistic approach might not be expected to be as high as classical relativistic scattering carried out numerically or a quantum, relativistic treatment. Fig. 4 compares these three treatments in the most extreme case, which is scattering off a uranium nucleus with 1000 hartree rescattering electrons. From the figure, one can see the yields differ at most by an order of magnitude and are within a factor of approximately three over much of the energy range. For lower Z species or rescattering energies less than 1000 hartree, the agreement between these three treatments will only improve. To be clear, for all calculations going forward in this study we will present the results using the relativistic quantum case. We show the comparison in Fig. 4 so the physics may be clear and to connect to classical models, which have been very successful in strong field interactions.

The second general finding addresses the overall yield of HHG near the ultimate energy limit across species of various atomic numbers, Z. While one could construct artificial fluences F_R, we present results consistent with the physics in Fig. 1 and Fig. 2. Thus, tunneling ionization serves as the electron source and relativistic propagation of the sourced electron probability gives rise to the fluence F_R used in the calculation of the scattering radiation. Even though very different species are ionizing, by adjusting the laser frequency and magnitude one can create very similar rescattering fluences (F_R) with tunneling ionization as the source for the rescattering electron.

Fig. 5 is a plot for uranium, krypton, and neon having tunneling ionization sourced rescattering fluences (see Fig. 5 caption for the laser conditions in each case). Fig. 5(a) gives the fluences for each case with a comparable F_R magnitude and cutoff energy at 500 hartree. Fig. 5(b) gives the energy-resolved bremsstrahlung radiation in each case. For all three atoms, the maximum HHG photon energy observed is the same. However, the bremsstrahlung yields differ by orders of magnitude between the three species. One can see in the figure the neon yield is a percent or so of that seen with uranium. Independent of the ion charge, the yield follows

closely to what is expected with a Z^2 scaling. This result is consistent with our understanding that interactions between the rescattering fluence and the nucleus are a close range, i.e. having impact parameters comparable to or smaller than the Bohr radius for the n=1 state for the ions.

Fig. 6 compares the current state of the art in HHG and the possible yields for rescattering with uranium with x-ray free electron laser sources. While normal optical and mid-IR lasers give maximum HHG energies of order 0.5 keV to 2 keV, one expects for uranium ionized by strong field, 38 nm wavelength radiation that HHG will extend out to 25 keV and have a yield fifty times higher (see Fig. 6(b)),

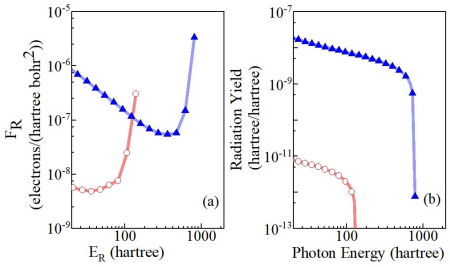

Figure 6. Numerical rescattering flux and resulting bremsstrahlung yields (Eq. 1) at $\Gamma_R = 1$ for U^{40+} (triangle, blue) at 5×10^{19} W/cm^2, $\lambda = 38nm$, and Ne^+ (empty circle, red) at 5×10^{14} W/cm^2, $\lambda = 5\mu m$. For clarity, symbols in the figure are for a reduced number of points. Lines in the graph are a linear connection of the full calculated result.

4. Conclusion

In conclusion, we show laser rescattering can access high energy, K- L_I-shell excitation across the periodic table from lithium to uranium. The optimized laser conditions for RSI follow a simple scaling as a function of the laser wavelength and atomic number. The result is promising in that laser rescattering across the periodic table may follow a predictable scaling for the ideal drive laser parameters. For the bremsstrahlung yields from laser-driven rescattering near the ultimate cutoff of HHG our findings show this regime can be accurately described as a semi-classical process where relativity must be included for the acceleration of the rescattering photoelectron but can be neglected when calculating the radiation from the collision. The radiation yield scales with the square of the nuclear charge, Z^2. Optimization of the rescattering fluence near the cutoff by using short laser drive wavelengths and high Z species like uranium gives a radiation yield with a photon cutoff out to the region of the one-thousand hartree ultimate cutoff with a yield 10^3 higher than from neon interacting with a strong field, mid-IR laser field. Taken together, it is clear that strong field rescattering processes are possible for all naturally occurring atoms. As a trend toward atoms with higher Z, the increase in energy scale pushes the ideal laser drive to shorter wavelengths. While traditional thought would consider long wavelength lasers in the mid-IR as better drivers of recattering, our study shows x-rays and modern free electron lasers are poised to extend strong field rescattering into new, heavy nuclei. In this new regime, deep inner shell excitations and high harmonic generation out to 30 keV are possible with yields orders of magnitude greater than possible with conventional optical or infra-red lasers.

Acknowledgments

This material is based upon work supported by the National Science Foundation under Grant No. 2133728 and 2110462.

References

[1] Corkum P 1993 *Physical Review Letters* **71** 1994

[2] Strickland D and Mourou G 1985 *Optics Communications* **56** 219
[3] Walser M, Keitel C, Scrinzi A and Brabec T 2000 *Physical Review Letters* **85** 5082
[4] Palaniyappan S, Ghebregziabher I, DiChiara A, MacDonald J and Walker B C 2006 *Physical Review A* **74** https://doi.org/10.1103/PhysRevA.74.033403
[5] Klaiber M, Hatsagortsyan K Z, Wu J, Luo S S, Grugan P and Walker B C 2017 *Physical Review Letters* **118** https://doi.org/10.1103/PhysRevLett.118.093001
[6] Kelley L, Germain Z, Jones E C, Milliken D and Walker B C 2021 *Journal of the Optical Society of America B-Optical Physics* **38** 3646 https://doi.org/10.1364/JOSAB.440211
[7] Jones E, Germain Z, Niessner J, Milliken D, Scilla J, Kelley L, MacDonald J and Walker B C 2021 *Physical Review A* **103** https://doi.org/10.1103/PhysRevA.103.023113
[8] Luo S S, Grugan P D and Walker B C 2014 *Journal of Physics B-Atomic Molecular and Optical Physics* **47**, https://doi.org/10.1088/0953-4075/47/13/135601
[9] Grugan P D, Luo S, Videtto M, Mancuso C and Walker B C 2012 *Physical Review A* **85** https://doi.org/10.1103/PhysRevA.85.053407
[10] Ammosov M V 1987 *Sov. Phys. JETP* **64** 1191
[11] Kramida A, Ralchenko Y, Reader J and Team N A (2020) *NIST Standard Reference Database* **78** Ver5.8 https://dx.doi.org/10.18434/T4W30F
[12] Ho P, Panfili R, Haan S and Eberly J 2005 *Physical Review Letters* **94** 093002 https://doi.org/10.1103/PhysRevLett.94.093002
[13] DiChiara A, Palaniyappan S, Falkowski A, Huskins E and Walker B 2005 *Journal of Physics B – Atomic Molecular and Optical Physics* **38** L183 https://doi.org/10.1088/0953-4075/38/10/L08
[14] DiChiara A D, Sistrunk E, Blaga C I, Szafruga U B, Agostini P and DiMauro L F, *Physical Review Letters* **108** https://doi.org/10.1103/PhysRevLett.108.033002 (2012).
[15] Palaniyappan S, DiChiara A, Ghebregziabher I, Huskins E L, Falkowski A, Pajerowski D and Walker B C 2006, *Journal of Physics B-Atomic Molecular and Optical Physics* **39** S357 https://doi.org/10.1088/0953-4075/39/13/S09
[16] Salvat F, Jablonski A and Powell C J 2005 *Computer Physics Communications* **165** 157
[17] Bethe H and Heitler W 1934 *Proceedings of the Royal Society of London Series A-Containing Papers of a Mathematical and Physical Character* **146** 0083